

## DISCOVERY OF A CIRCUMBINARY DISK AROUND HERBIG AE/BE SYSTEM V892 TAU

J. D. MONNIER<sup>1</sup>, A. TANNIRKULAM<sup>1</sup>, P. G. TUTHILL<sup>2</sup>, M. IRELAND<sup>2</sup>, R. COHEN<sup>3</sup>, W. C. DANCHI<sup>4</sup>, F. BARON<sup>5</sup>

*Accepted for publication in ApJ Letters*

### ABSTRACT

We report the discovery of a circumbinary disk around the Herbig Ae/Be system v892 Tau. Our detailed mid-infrared images were made using segment-tilting interferometry on the Keck-1 Telescope and reveal an asymmetric disk inclined at  $\sim 60^\circ$  with an inner hole diameter of 250 mas (35 AU), approximately  $5\times$  larger than the apparent separation of the binary components. In addition, we report a new measurement along the binary orbit using near-infrared Keck aperture masking, allowing a crude estimate of orbital parameters and the system mass for the first time. The size of the inner hole appears to be consistent with the minimum size prediction from tidal truncation theory, bearing a resemblance to the recently unmasked binary CoKu Tau/4. Our results have motivated a re-analysis of the system spectral energy distribution, concluding the luminosity of this system has been severely underestimated. With further study and monitoring, v892 Tau should prove a powerful testing ground for both predictions of dynamical models for disk-star interactions in young systems with gas-rich disks and for calibrations of pre-main-sequence tracks for intermediate-mass stars.

*Subject headings:* techniques:interferometric, stars: pre-main sequence, stars: binaries: close, infrared:stars, stars: individual (v892 Tau)

### 1. INTRODUCTION

v892 Tau (Elias-1, Elias 3-1) is a young stellar object in the Taurus-Aurigae star forming region ( $d = 140 pc$ , Kenyon et al. 1994). Its visible spectrum is classified as spectral type B8V (Hernández et al. 2004), making v892 Tau one of the few Herbig Ae/Be stars in Taurus (in addition to AB Aur, MWC 480). The spectral energy distribution (SED) of v892 Tau is dominated by bright thermal emission in the mid-infrared (Hillenbrand et al. 1992), with relatively large line-of-sight extinction in the visible (one estimate is  $A_V \sim 5.9$ , Kenyon & Hartmann 1995). Despite being one of the closest Herbig stars and after decades of multi-wavelength observations, the nature of v892 Tau is still uncertain.

The SED suggests v892 Tau is either a young embedded Class I source (Lada 1987) still surrounded by its nascent envelope or a more evolved, Class II object (i.e., Herbig Ae/Be star) seen through its edge-on disk. Spatially-resolved imaging can easily distinguish between these two scenarios, and early speckle interferometry (Kataza & Maihara 1991; Haas et al. 1997; Leinert et al. 2001) suggested the presence of an extended and elongated nebula in the near-infrared that could be due to scattering in bipolar lobes.

The high-resolution speckle imaging of Smith et al. (2005) clearly resolved the K band ( $\lambda = 2.2\mu m$ ) emission to be coming from two unresolved stars in v892 Tau with little or no sign of a nebula or extended emission. The two stars of roughly equal brightness had an apparent separation of 55 milliarcseconds (7.7 AU) and some evidence of orbital motion was seen between epochs sep-

arated by 7 years.

Although this binary should have a dramatic effect on the infrared emission, carving out a large hole in the circumbinary disk, recent analysis of the SED of v892 Tau including ISO data (Acke & van den Ancker 2004) uncovered no distinct signature of the underlying binary<sup>6</sup>. Other workers (Liu et al. 2005, 2007) made use of the technique of nulling interferometry in the mid-IR ( $\lambda = 10.3\mu m$ ) to marginally resolve v892 Tau (FWHM  $\sim 20 AU$ ) along PA  $164^\circ$  consistent with normal (single-star) disk emission.

Here, we report new mid-IR imaging of the v892 Tau system which resolves these mysteries, discovering very extended and resolved emission that we interpret to be coming from a circumbinary disk. We also confirm the presence of the binary at K band and our new data allow first crude estimates of the orbital elements. Lastly, we report a new SED analysis which provides an improved determination of the system luminosity and our viewing geometry.

### 2. OBSERVATIONS

We observed v892 Tau using the Keck-1 telescope as part of two separate experiments, the Keck segment-tilting experiment and the Keck aperture masking experiment. Here, we briefly describe these experiments and give pertinent observing details.

v892 Tau was observed on UT2004Aug31, UT 2004Sep01, and UT2005Feb19 at the Keck-1 telescope using the  $10.7\mu m$  filter ( $\lambda_0 = 10.7\mu m$ ,  $\Delta\lambda = 1.55\mu m$ ) of the Long Wavelength Spectrometer (LWS, Campbell & Jones 2004) just before this instrument was decommissioned in 2005. In order to optimize our calibration against changes in seeing (e.g., Tuthill et al. 2000), we used the Keck's segmented primary mirror in a novel "segment-tilting" mode, whereby

<sup>6</sup> Acke & van den Ancker (2004) did note strong  $11.2\mu m$  PAH emission and anomalous infrared colors.

Electronic address: JDM: monnier@umich.edu

<sup>1</sup> monnier@umich.edu: University of Michigan Astronomy Department, 941 Dennison Bldg, Ann Arbor, MI 48109-1090, USA.

<sup>2</sup> University of Sydney

<sup>3</sup> W. M. Keck Observatory

<sup>4</sup> NASA-GSFC

<sup>5</sup> University of Cambridge

we controlled the tilts and pistons of the individual mirror segments to create a set of 4 independent and non-redundant interference patterns (using 6 segments each) on the LWS detector focal plane. Furthermore, short exposures were used ( $t_{\text{int}} = 90 \text{ ms} < t_0$ , where  $t_0$  is the atmospheric coherence time  $\sim 250 \text{ ms}$  in the mid-IR) to effectively freeze the atmospheric turbulence. For calibration we interleaved target observations with calibrators  $\alpha$  Tau<sup>7</sup>,  $\iota$  Aur, and  $\alpha$  Cet. Details on this experiment and the implementation at Keck were first introduced by Monnier et al. (2004) and more information can be found in recently published science papers (Weiner et al. 2006; Ireland et al. 2007; Rajagopal et al. 2007).

The combined Fourier coverage of the four patterns over the three nights (total of 6 independent pointings) can be found in Figure 1 along with the visibility results. The visibility-squared data and the closure phases were compiled and saved using the OIFITS data format (Pauls et al. 2005) and are available upon request. Figure 1 shows the clear sign of highly-elongated disk emission.

We also obtained diffraction-limited observations of v892 Tau in the near-IR on UT2004Sep04 using the K-band filter ( $\lambda = 2.21 \mu\text{m}$ ,  $\Delta\lambda = 0.43 \mu\text{m}$ ) of the NIRC camera (Matthews et al. 1996) in conjunction with an annulus aperture mask placed in front of the secondary mirror. This observing mode was extensively utilized between 1997 and 2005 (see most recent science papers, Monnier et al. 2007; Tuthill et al. 2008) and details of the experimental design and performance can be found in Tuthill et al. (2000). We interleaved observations of the target with the unresolved calibrator 54 Per. The Fourier coverage and visibility-squared results are shown in Figure 1, where the the binary nature is clearly revealed.

### 3. ANALYSIS

#### 3.1. Image Reconstructions

We used the BSMEM image reconstruction software (Buscher 1994; Lawson et al. 2004, 2006) for aperture synthesis imaging. Figure 2 shows the reconstructed images for the mid-IR and near-IR data. In order to confirm the asymmetric features in the mid-IR image were not due to artifacts in the BSMEM algorithm, we also used the independent image reconstruction code MACIM (Ireland et al. 2006) and found good consistency between the basic morphology, size scale, and level of emission asymmetry. As an additional data quality check, separate images were made for each independent night of data and the resulting images all closely resembled the result shown in Figure 2. Note that we do not know the relative position of the near-IR image compared to mid-IR image and have presented each image centered in its corresponding frame.

##### 3.1.1. Mid-infrared: Elongated disk structure

The mid-IR image shows elongated emission, approximately 320 mas by 180 mas in full extent, elongated along PA 50°. The two bright lobes in the image are separated by 210 mas (30 AU) with the south-west side being significantly brighter. A two-dimensional Gaussian fit to the

visibility data gives a FWHM  $244 \pm 6 \text{ mas} \times 123 \pm 9 \text{ mas}$  along PA  $49 \pm 1^\circ$ . For a simplistic “flat disk” model, this 2-to-1 ratio elongation suggests we are viewing this disk oriented at  $\gtrsim 60^\circ$  inclination.

A more suitable model for a circumbinary or transitional disk would be a tilted and asymmetric ring of emission that is nearly unresolved along the minor axis (for example, see dramatic case of HR 4796; Koerner et al. 1998; Schneider et al. 1999). Following the parameterization of Monnier et al. (2006), we have fitted a “skewed asymmetric ring model” to our interferometry data here to better estimate the inner hole diameter. The best fitting model had an inner-hole diameter of  $247 \times 121 \text{ mas}$  ( $35 \times 17 \text{ AU}$ ) along PA  $53^\circ$ , with a 40% skew along PA  $284^\circ$  (the thickness of the ring followed a gaussian profile with a FWHM of 25% ring radius). For purposes of §4, we will assume the central hole in the circumbinary disk has a radius of 17.5 AU.

Importantly, we want to emphasize that the scale of the emission is more than  $4\times$  larger than the separation of the binary at the heart of this system, and the elongation is along a distinctly-different position angle. Since our mid-IR data in 2004 were taken within one week of the near-IR data, we can clearly prove that the elongated mid-IR emission comes from a distinct and much larger component than the near-IR. We discuss the relationship between the circumbinary disk and the underlying binary orbit in §4.

At first glance, it may seem surprising that Liu et al. (2005) did not more clearly resolve this large circumbinary disk using their nulling technique, finding a FWHM of only 20 AU. However, this nulling measurement was performed only for PA  $164^\circ$ , which is along the narrow dimension of the elongated emission we detected. Another possible explanation for the smaller size is that the band-pass filter used here has more contribution from  $11.2 \mu\text{m}$  PAH emission, which could be more extended than the mid-IR continuum.

##### 3.1.2. Near-infrared: Binary star

Figure 2 shows the BSMEM image of v892 Tau at  $2.2 \mu\text{m}$ . We confirm the binary nature of this target as first reported by Smith et al. (2005). We also set a limit of  $<10\%$  of the emission possibly coming from any sort of extended or “halo” component (e.g., Kataza & Maihara 1991; Haas et al. 1997; Leinert et al. 2001). In order to extract the separation and position angle of this binary, we have used both image fitting and direct fitting to the interferometric observables to yield the following result:  $\rho = 44.2 \pm 1.0 \text{ mas}$ ,  $\theta = 79.9 \pm 1.0^\circ$ , Flux Ratio  $1.15 \pm 0.04$  (west component brighter than east component).

##### 3.2. Binary orbit

We combined our new binary measurement (at 2004.67) with the 1996.75 and 2003.76 measurements from Smith et al. (2005) and these data are plotted in Figure 3. The small proper motion ( $\Delta \sim 10 \text{ mas} = 1.4 \text{ AU}$ ) observed by Smith et al. (2005) over 7 years is problematic for this object since this would require a long period orbit ( $\gtrsim 100 \text{ yrs}$ ) inconsistent with the spectral types and luminosities of the binary stars themselves.

Alternatively, the binary period could be approximately 7 years, meaning the stars had gone nearly exactly once around their orbit between epochs. Although

<sup>7</sup> All calibrators were assumed unresolved except  $\alpha$  Tau where we adopted a uniform disk diameter of 19.8 mas (Perrin et al. 1998).

the timing is suspicious, the scenario is plausible except this would require a system mass  $>20 M_{\odot}$ , much too high for the B8 spectral type and system luminosity.

The scenario we favor is that infrared variability affected the brightness ratio between 1996 and 2003, confusing the assignment of “primary” and “secondary” star. This variation could be intrinsic or be due to varying line-of-sight obscuration through this asymmetric disk. Smith et al. (2005) did report a change in flux ratio, finding a brightness ratio of 1.0 for 2003.76 which implies that their reported position angle had a  $\pm 180^{\circ}$  ambiguity.

In our 2004.67 data, we definitively detect the southwest component as 15% brighter, consistent with the PA assignment of the published 2003.76 measurement. By flipping the position angle of the earlier 1996 measurements, we find a robust family of orbits with periods of  $\sim 14$  years, compatible with the measured binary separations and the expected system mass. Note that future orbital refinement will lead to precise stellar masses for these intermediate-mass, pre-main-sequence stars (see also MWC 361A, Monnier et al. 2006) – a rare opportunity to advance the calibration of pre-main-sequence tracks for this mass range.

To estimate the orbital parameters for v892 Tau, we used Monte Carlo sampling of the measured stellar separations along with a system mass constraint of  $5.5 \pm 0.5 M_{\odot}$  expected for two stars of spectral type B8V (Palla & Stahler 1993). Figure 3 shows the main results of our orbital study:  $P = 13.8 \pm 1.5$  yrs,  $a = 72.4 \pm 6.3$  mas (10 AU),  $e = 0.12 \pm 0.05$ ,  $i = 60.6 \pm 3.8^{\circ}$ ,  $\omega = 233 \pm 42^{\circ}$ ,  $\Omega = 28 \pm 5^{\circ}$ ,  $T_O = 55480 \pm 900$  MJD.

#### 4. DISCUSSION

We interpret the mid-IR emission of v892 Tau as a circumbinary disk based on several arguments. The mid-IR emitting region is much larger than the separation between the binary components, ruling out models which have all the mid-IR emission coming from disks around the individual stars. In theoretical models of tidal truncation (Artymowicz & Lubow 1994), the circumbinary disk has an inner hole approximately  $1.8\text{--}2.6\times$  larger than the semi-major axis of the binary system (for eccentricity between 0 and 0.25). For comparison, our best estimates of the hole radius and orbital semi-major axis are 17.5 AU and 10 AU respectively – giving a ratio of 1.75 which is close to the theoretical expectation. Additionally, the position angle and derived inclination angle of the mid-IR emission ( $PA \sim 50^{\circ}$ ,  $i \sim 60^{\circ}$ ) is similar to those derived from the orbit ( $PA \sim 28^{\circ}$ ,  $i \sim 61^{\circ}$ ) and the mild asymmetry in the mid-IR emission suggests dynamical interactions between an eccentric binary and the surrounding disk (via resonances or disk warping).

We further test the circumbinary disk hypothesis by analyzing the spectral energy distribution (SED). The SED shows a large mid-IR bump similar to that seen in “transitional” disks (Calvet et al. 2002; Espaillat et al. 2007). By reddening template Kurucz spectra for B8V stars, we can fit the near-IR emission with mostly photospheric light (some near-IR emission from hot dust is allowed but not well constrained) assuming  $A_V = 10.95$  yielding a combined stellar luminosity of  $400 L_{\odot}$ , reasonable for two B8V stars. Our new proposed SED decomposition for v892 Tau can be found in Figure 3, showing that the rising mid-IR flux can be roughly characterized

as a  $T \sim 450$  K blackbody, consistent with emission from the warm inner wall of the circumbinary disk.

Using equation (1) in Isella et al. (2006), the predicted radius for the warm inner wall for the above stellar luminosity (assuming  $0.25 \mu\text{m}$  spherical silicate grains) is 18 AU – consistent with our derived inner hole radius of 17.5 AU based on imaging. Furthermore, we find that the scale height of this wall at 18 AU is  $\sim 1.8$  AU (Dullemond et al. 2001) which can produce the observed line-of-sight  $A_V \sim 11$  for the disk inclination of  $\sim 65^{\circ}$ . This latter phenomena may not be widely appreciated – circumbinary (or transitional) disks have warm puffed-up inner walls (the rim scale height is a stronger function of radius than temperature) at large radii that effectively increases the possibility that central stars will be obscured or at least reddened as seen by distant observers. The lack of scattering nebulosity in archival Hubble Space Telescope images independently suggests that the high line-of-sight  $A_V$  is likely from absorption by dust in the outer disk and not infalling envelope material. While a detailed model is beyond the scope of this Letter, a careful study will allow precise constraints of stellar luminosities, dust properties, and circumbinary structure and should be straight-forward with today’s 3-D Monte Carlo radiative transfer codes (e.g., TORUS, Harries 2000).

#### 5. CONCLUSIONS

We have discovered an extensive circumbinary disk around v892 Tau in the mid-infrared. We also independently confirm the binary nature of the underlying stellar system and our new measurement allows us to fit an astrometric orbit, finding a period  $\sim 14$  years for system mass of  $\sim 6 M_{\odot}$ . Our limited orbital phase coverage and some ambiguity in position angles allow only crude estimates and we strongly urge continued monitoring of this system using near-IR speckle, aperture masking, or adaptive optics.

We have proposed a new SED decomposition with a line-of-sight extinction ( $A_V \sim 11$ ) higher than previously thought, implying a system luminosity  $\sim 400 L_{\odot}$ . This result highlights the fact that circumbinary disks (and transitional disks) have much larger opening angles since the puffed-up inner wall causes enhanced extinction of the central stars even at inclinations of  $60^{\circ}$ .

v892 Tau is another case where high-resolution imaging has motivated a fundamental shift in our understanding of an individual object. As spectral energy distributions are used to discover “transitional” disks implicating planet formation, we must be cognizant of the important role of binarity and the associated circumbinary disks that can mimic signs of planet formation (e.g., Ireland & Kraus 2008). Far from merely being spoilers to planet finders, new circumbinary disks offer fresh laboratories for studying dynamical interactions between gas-rich disks and the massive orbiting bodies embedded within them as well as critical opportunities to calibrate pre-main sequence tracks.

We thank Nuria Calvet and Jesus Hernandez for helpful discussions and acknowledge support from NASA KPDA grant 1267021, NASA Origins grant NNG05GI80G, nsf-ast 0352728, and the NASA Michelson Fellowship program (MJI). The data presented

herein were obtained at the W.M. Keck Observatory, which is operated by Caltech, University of California and NASA. WMKO was made possible by the financial support of the W.M. Keck Foundation. The authors wish to recognize and acknowledge the very significant cul-

tural role and reverence that the summit of Mauna Kea has always had within the indigenous Hawaiian community. We are most fortunate to have the opportunity to conduct observations from this mountain.

*Facility:* Keck:I (LWS,NIRC) Hiltner (TIFKAM)

#### REFERENCES

- Acke, B. & van den Ancker, M. E. 2004, *A&A*, 426, 151  
 Artymowicz, P. & Lubow, S. H. 1994, *ApJ*, 421, 651  
 Buscher, D. F. 1994, in *IAU Symposium*, Vol. 158, Very High Angular Resolution Imaging, ed. J. G. Robertson & W. J. Tango, 91+  
 Calvet, N., D'Alessio, P., Hartmann, L., Wilner, D., Walsh, A., & Sitko, M. 2002, *ApJ*, 568, 1008  
 Campbell, R. D. & Jones, B. 2004, *Advances in Space Research*, 34, 499  
 Dullemond, C. P., Dominik, C., & Natta, A. 2001, *ApJ*, 560, 957  
 Espaillat, C., et al. 2007, *ApJ*, 670, L135  
 Haas, M., Leinert, C., & Richichi, A. 1997, *A&A*, 326, 1076  
 Harries, T. J. 2000, *MNRAS*, 315, 722  
 Herbst, W. & Shevchenko, V. S. 1999, *AJ*, 118, 1043  
 Hernández, J., Calvet, N., Briceño, C., Hartmann, L., & Berlind, P. 2004, *AJ*, 127, 1682  
 Hillenbrand, L. A., Strom, S. E., Vrba, F. J., & Keene, J. 1992, *ApJ*, 397, 613  
 Ireland, M. J. & Kraus, A. L. 2008, *ApJ*, 678, L59  
 Ireland, M. J., Monnier, J. D., & Thureau, N. 2006, *Proceedings of SPIE*, Vol. 6268, pp. 62681T  
 Ireland, M. J., et al. 2007, *ApJ*, 662, 651  
 Isella, A., Testi, L., & Natta, A. 2006, *A&A*, 451, 951  
 Kataza, H. & Maihara, T. 1991, *A&A*, 248, L1  
 Kenyon, S. J., Dobrzycka, D., & Hartmann, L. 1994, *AJ*, 108, 1872  
 Kenyon, S. J. & Hartmann, L. 1995, *ApJS*, 101, 117  
 Koerner, D. W., Ressler, M. E., Werner, M. W., & Backman, D. E. 1998, *ApJ*, 503, L83+  
 Lada, C. J. 1987, in *IAU Symposium*, Vol. 115, Star Forming Regions, ed. M. Peimbert & J. Jugaku, 1–17  
 Lawson, P. R., et al. 2006, *Proceedings of SPIE*, Vol. 6268, pp. 62681U  
 Lawson, P. R., et al. 2004, *Proceedings of SPIE*, Vol. 5491, p.886  
 Leinert, C., Haas, M., Abraham, P., & Richichi, A. 2001, *A&A*, 375, 927  
 Liu, W. M., et al. 2005, *ApJ*, 618, L133  
 Liu, W. M., et al. 2007, *ApJ*, 658, 1164  
 Matthews, K., Ghez, A. M., Weinberger, A. J., & Neugebauer, G. 1996, *PASP*, 108, 615+  
 Monnier, J. D., et al. 2006, *ApJ*, 647, 444  
 Monnier, J. D., et al. 2007, *ApJ*, 655, 1033  
 Monnier, J. D., Tuthill, P. G., Ireland, M. J., Cohen, R., & Tannirkulam, A. 2004, in *Bulletin of the AAS*, Vol. 36, 1367+  
 Palla, F. & Stahler, S. W. 1993, *ApJ*, 418, 414  
 Pauls, T. A., Young, J. S., Cotton, W. D., & Monnier, J. D. 2005, *PASP*, 117, 1255  
 Perrin, G., et al. Coude Du Foresto, V., Ridgway, S. T., Mariotti, J.-M., 1998, *A&A*, 331, 619  
 Rajagopal, J., et al. 2007, *ApJ*, 671, 2017  
 Schneider, G., et al. 1999, *ApJ*, 513, L127  
 Smith, K. W., et al. 2005, *A&A*, 431, 307  
 Strom, K. M. & Strom, S. E. 1994, *ApJ*, 424, 237  
 Tuthill, P. G., et al. 2000, *PASP*, 112, 555  
 Tuthill, P. G., et al. 2008, *ApJ*, 675, 698  
 Weiner, J., et al. 2006, *ApJ*, 636, 1067

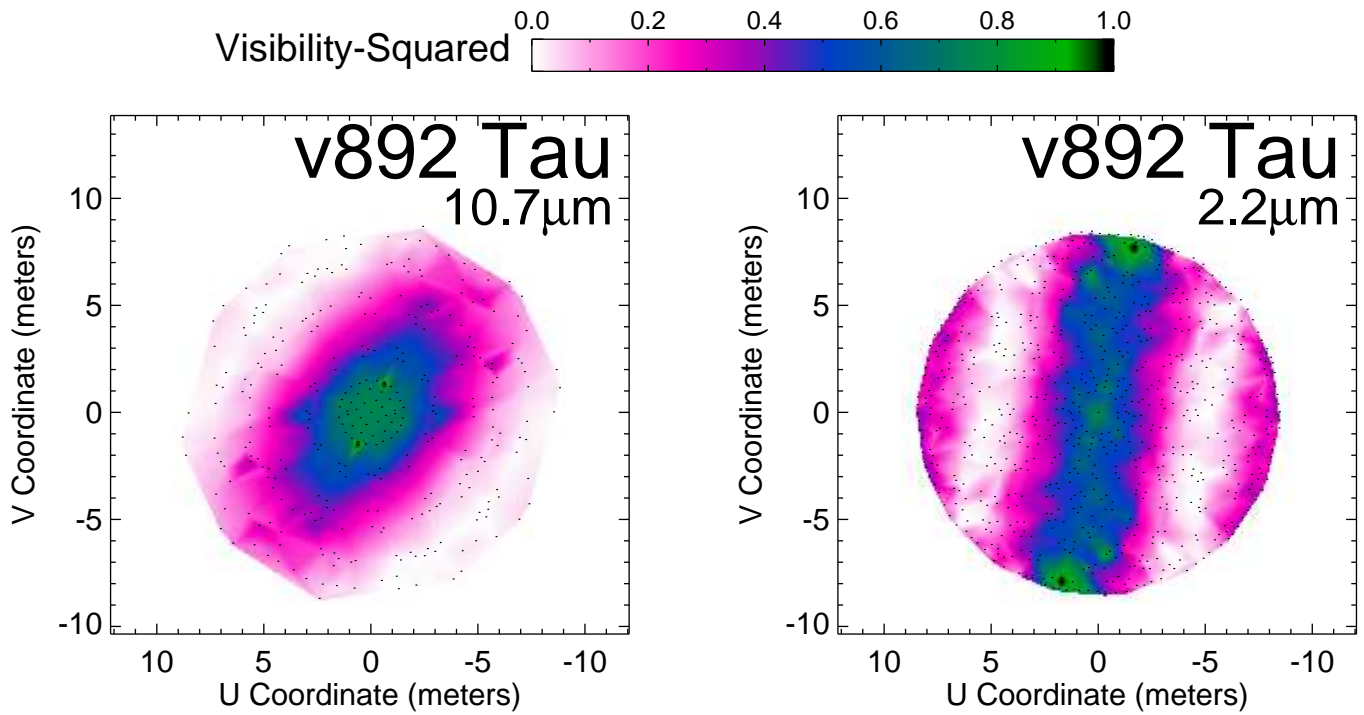


FIG. 1.— This figure shows visibility data (color scale) for v892 Tau and the specific Fourier coverage (dots). The left panel shows results for 10.7 $\mu$ m using the Keck segment tilting method while the right panel applies to the 2.2 $\mu$ m Keck aperture masking data.

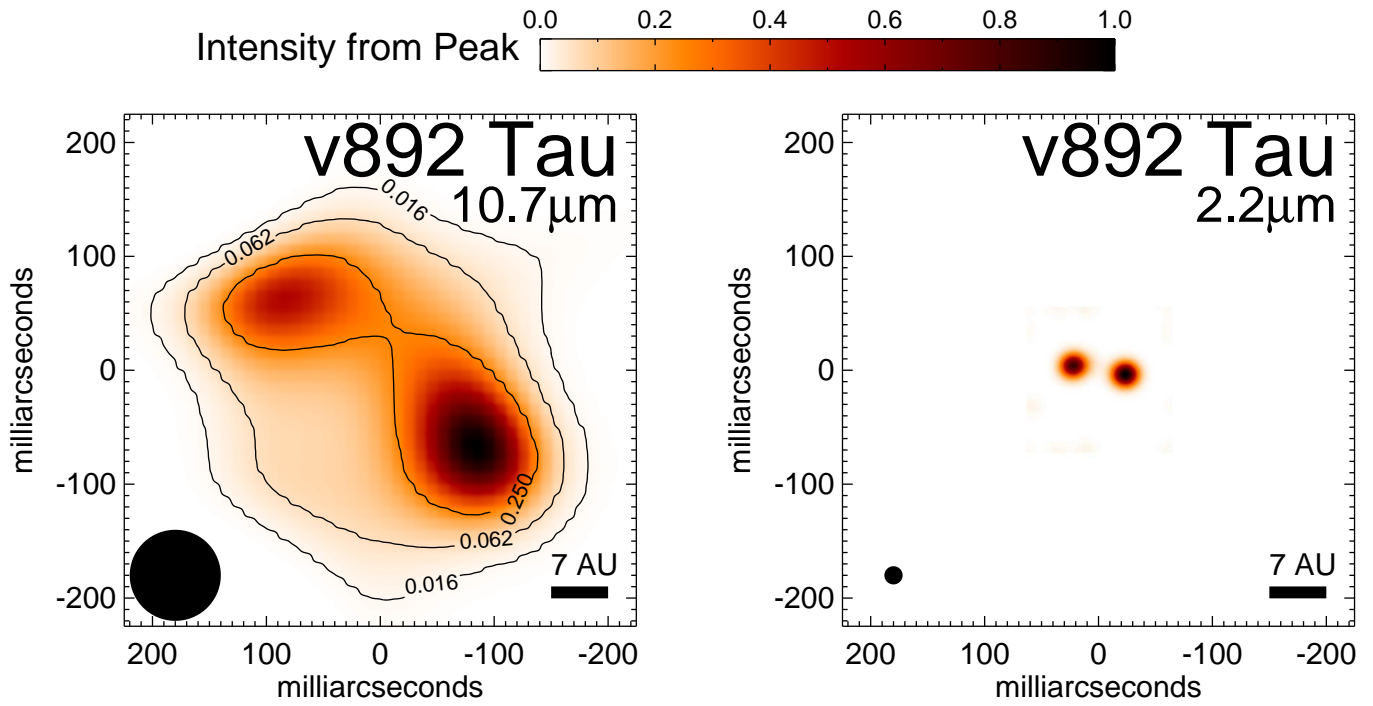


FIG. 2.— This figure shows the image reconstructions of v892 Tau at  $10.7\mu\text{m}$  (left panel) and  $2.2\mu\text{m}$  (right panel) using the BSMEM software. At the bottom-left of each panel, we have included an estimate of the resolution of each image, corresponding here to 80 mas at  $10.7\mu\text{m}$  and 16 mas at  $2.2\mu\text{m}$ . Contour levels are shown for the extended emission in the mid-IR spaced logarithmically in factors of 4: 25%, 6.3%, and 1.6% of the peak. The scale bar applies for a distance of 140 pc. For orientation, East points left and North points up.

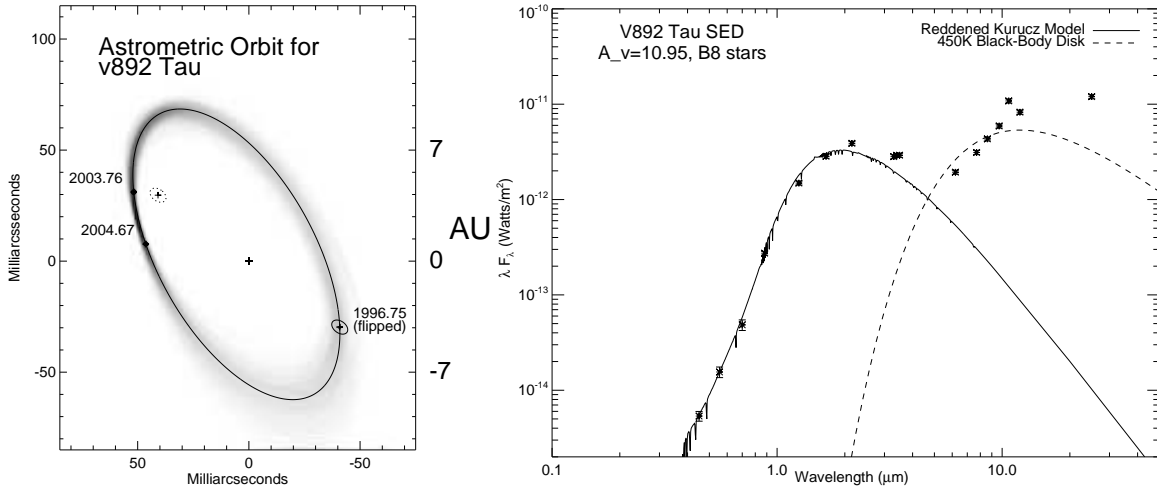


FIG. 3.— (*left panel*) This figure shows the separation and position angle measurements for  $\nu$ 892 Tau from Smith et al. (2005) and this work. We have plotted the best-fit model for a system mass of  $5.5 M_\odot$  (period 13.8 yrs, eccentricity 0.12) with the solid curve. Note that we had to flip the position angle of the 1996 epoch measurement in order to find a realistic orbit (see §3.2 for full description of our procedure and justification). (*right panel*) This figure shows the spectral energy distribution for  $\nu$ 892 Tau (photometry from Strom & Strom 1994; Acke & van den Ancker 2004; Herbst & Shevchenko 1999, and our own JHK photometry from MDM Observatory) and our proposed decomposition of star plus disk. We have plotted the contribution from the reddened ( $A_V = 10.95$ ,  $R_V = 6.4$ ) stellar photospheres ( $2 \times B8V$ , system luminosity of  $400 L_\odot$ ) and the contribution from the “warm inner wall” of the circumbinary disk with temperature  $T \sim 450K$ .